Grating-free Raman laser using highly nonlinear photonic crystal fiber

S. Randoux[1], N. Y. Joly[1], G. Mélin[2], A. Fleureau[2], L. Galkovsky[2], S. Lempereur[2], and P. Suret[1]

[1] *Laboratoire de Physique des Lasers, Atomes et Molécules, UMR CNRS 8523, Centre d' Etudes et de Recherches Lasers et Applications, Université des Sciences et Technologies de Lille, F-59655 Villeneuve d'Ascq, France*

[2] *Draka Comteq, route de Nozay, 91460 Marcoussis, France*

stephane.randoux@univ-lille1.fr

Abstract: We demonstrate a Raman laser made from a grating-free highly-nonlinear photonic crystal fiber. The laser threshold power is lower than 600 mW and laser power characteristics recorded in experiments are accurately described from the usual simplest model dealing only with stationary evolutions of total optical powers [J. Opt. Soc. Am. **69**, 803–807 (1979)]. In our theoretical treatment, reflectivity coefficients are fixed parameters, in strong contrast with procedures usually implemented to describe Raman fiber lasers made with fiber Bragg gratings. Experimental investigations of the spectral properties of our grating-free Raman fiber laser evidence that the shape of the Stokes power spectrum remains remarkably Gaussian whatever the incident pump power. Increasing the incident pump power induces a drift of the Stokes wavelength together with a broadening of the Stokes optical spectrum. Investigations on the role of light polarization on laser characteristics show that our grating-free Raman fiber laser behaves as a Raman laser made with a standard polarization maintaining fiber.

© 2007 Optical Society of America

OCIS codes: (140.3550) Lasers, Raman (140.3510) Lasers, fiber (160.2290) Fiber materials

References and links

1. M. D. Mermelstein, C. Headley, J.-C. Bouteiller, P. Steinvurzel, C. Horn, K. Feder, and B. J Eggleton, "Configurable three-wavelength Raman fiber laser for Raman amplification and dynamic gain flattening," IEEE Photon. Technol. Lett. **13,** 1286-1288 (2001).
2. F. Vanholsbeeck, S. Coen, P. Emplit, C. Martinelli, and T. Sylvestre, "Cascaded Raman generation in optical fibers: influence of chromatic dispersion and Rayleigh backscattering," Opt. Lett. **29,** 998–1000 (2004).
3. B. A. Cumberland, S. V. Popov, J. R. Taylor, O. I. Medvedkov, S. A. Vasiliev, and E. M. Dianov, "2.1 μm continuous-wave Raman laser in GeO_2 fiber," Opt. Lett. **32,** 1848–1850 (2007).
4. D. A. Chestnut and J. R. Taylor, "Wavelength-versatile subpicosecond pulsed lasers using Raman gain in figure-of-eight fiber geometries," Opt. Lett. **30,** 2982–2984 (2005).
5. P. Yan, S. Ruan, C. Guo, Y. Yu, and L. Li, "Efficient, tunable photonic crystal fiber Raman laser," Microwave Opt. Technol. Lett. **49,** 395–397 (2007).
6. Y. Zhao and S. D. Jackson, "Highly efficient free running cascaded Raman fiber laser that uses broadband pumping," Opt. Express **13,** 4731–4736 (2005).
7. C. A. Codemard, P. Dupriez, Y. Jeong, J. K. Sahu, M. Ibsen, and J. Nilsson, "High-power continuous-wave cladding-pumped Raman fiber laser," Opt. Lett. **31,** 2290–2292 (2006).
8. Y. Zhao and S. D. Jackson, "Highly efficient first order Raman fibre lasers using very short Ge-doped silica fibres," Opt. Commun. **253,** 172–176 (2005).

#86993 - $15.00 USD Received 28 Aug 2007; revised 3 Oct 2007; accepted 3 Oct 2007; published 19 Nov 2007

9. J.C. Travers, S. V. Popov, and J. R. Taylor, "Efficient continuous-wave holey fiber Raman laser," Appl. Phys. Lett. **87,** 031106 (2005).
10. Z. Xiong, N. Moore, Z. G. Li, and G. C. Lim, "10-W Raman Fiber Lasers at 1248 nm Using Phosphosilicate Fibers," IEEE J. Lightwave Technol. **21,** 2377–2381 (2003).
11. J. AuYeung and A. Yariv, "Theory of cw Raman oscillation in optical fibers," J. Opt. Soc. Am. **69,** 803–807 (1979).
12. S. A. Babin, D. V. Churkin, and E. V. Podivilov, "Intensity interactions in cascades of a two-stage Raman fiber laser," Opt. Commun. **226,** 329–335 (2003).
13. M. Krause, S. Cierullies, and H. Renner, "Stabilizing effect of line broadening in Raman fiber lasers" Opt. Commun. **227,** 355–361 (2003).
14. J. C. Bouteiller, "Spectral modeling of Raman fiber lasers," IEEE Photon. Technol. Lett. **15,** 1698–1700 (2003).
15. R. Vallée, E. Bélanger, B. Déry, M. Bernier, and D. Faucher, "Highly efficient and high-power Raman fiber laser based on broadband chirped fiber Bragg gratings," IEEE J. Lightwave Technol. **24,** 5039–5042 (2006).
16. P. Suret and S. Randoux, "Influence of spectral broadening on steady characteristics of Raman fiber lasers: from experiments to questions about the validity of usual models," Opt. Commun. **237,** 201–212 (2004).
17. R. H .Stolen, "Polarization effects in fiber Raman and Brillouin lasers," IEEE J. Quantum Electron. **QE-15,** 1157–1160 (1979).
18. S. Randoux, A. Doutté, and P. Suret, "Polarization-resolved analysis of the characteristics of a Raman laser made with a polarization maintaining fiber," Opt. Commun. **260,** 232–241 (2006).
19. S. A. Babin, D. V. Churkin, A. E. Ismagulov, S. I. Kablukov, and E. V. Podivilov, "Spectral broadening in Raman fiber lasers," Opt. Lett. **31,** 3007–3009 (2006).
20. S. A. Babin, D. V. Churkin, A. E. Ismagulov, S. I. Kablukov, and E. V. Podivilov, "Four-wave-mixing-induced turbulent spectral broadening in a long Raman fiber laser," J. Opt. Soc. Am. B **24,** 1729–1738 (2007).
21. R. H. Stolen, C. Lee, and R. K. Jain, "Development of the stimulated Raman spectrum in single-mode silica fibers," J. Opt. Soc. Am. B **1,** 652–657 (1984).
22. A. Doutté, P. Suret, and S. Randoux, "Influence of light polarization on dynamics of continuous-wave-pumped Raman fiber lasers," Opt. Lett. **28,** 2464–2466 (2003).
23. S. A. Skubchenko, M. Y. Vyatkin, and D. V. Gaspontsev, "High-Power CW Linearly Polarized All-Fiber Raman Laser," IEEE Photon. Technol. Lett. **16,** 1014–1016 (2004).
24. L. Labonté, D. Pagnoux, P. Roy, F. Bahloul, and M. Zghal, "Numerical and experimental analysis of the birefringence of large air fraction slightly unsymmetrical holey fibres," Opt. Commun. **262,** 180–187 (2006).

1. Introduction

Continuous-wave pumped Raman all-fiber lasers are versatile light sources which are now virtually able to deliver high-power radiation at any wavelength across the $1-2.1\ \mu$m spectral region [1–3]. Numerous cavity geometries have been investigated so far and Raman fiber lasers (RFLs) have been shown to exhibit many attractive capabilities such as multiwavelength operation, pulsed emission or tunability [4–6]. Various fibers have also been designed to strengthen nonlinearities and RFLs are now able to deliver cw optical powers as high as ~ 10 Watt [7–10].

In their simplest and most popular configuration, RFLs oscillate within a Fabry-Perot cavity which is closed by two fiber Bragg gratings (FBGs). Broadening of the optical spectrum and influence of light polarization are among the most important issues which have been examined in these lasers during the past few years. Briefly synthesizing approaches commonly found, both spectral broadening and polarization effects are often treated within the framework of the model introduced by AuYeung and Yariv in the 1970's [11].

Spectral broadening is very often treated by introducing an "effective reflectivity" R_{eff} which describes phenomenologically the fact that the laser optical spectrum becomes wider than the reflectivity spectrum of the FBGs [12–15]. With models phenomenologically modified in this way, the reflectivity coefficients R of the cavity mirrors become either arbitrarily fixed parameters ($R = R_{eff}$) either variable functions of incident pump power ($R = R_{eff}(P_{inc})$) [15]. Although this kind of procedure actually provides characteristics fitting well experimental curves [15], the introduction of an effective reflectivity has no physical significance [16].

Since the role of light polarization is ignored in the simple scalar model introduced in ref. [11], polarization effects occurring in RFLs are often treated from the argumentation initially developed by Stolen in 1979 [17]. Following Stolen, mismatch between the states of

#86993 - $15.00 USD Received 28 Aug 2007; revised 3 Oct 2007; accepted 3 Oct 2007; published 19 Nov 2007
(C) 2007 OSA

polarization of pump and Stokes waves induces a reduction of the Raman gain integrated over the fiber length. Threshold doubling occurring in Raman lasers made with polarization maintaining fibers (PMFs) is thus commonly explained from a reduction by a factor 2 of the Raman gain coefficient [9].

In summary, the physics of RFLs is nowadays commonly described from the model introduced by AuYeung and Yariv in 1979. Effects that cannot be ignored in "real-life" RFLs (spectral broadening and polarization effects) are very often treated by phenomenological adjustements of physical parameters. It should be emphasized that a quantitative agreement between experiments and predictions from the usual model has never been found so far without such phenomenological adjustments.

In this paper, we demonstrate for the first time to our knowledge a RFL exhibiting characteristics that can be described in an accurate and quantitative way from the model introduced by AuYeung and Yariv without any phenomenological adjustment of physical parameters. Our laser is made from a 220−m long highly nonlinear photonic crystal fiber (HN-PCF) which provides Raman gain sufficiently high to observe Stokes emission without FBGs at a threshold power of only ~ 600 mW. It oscillates within a Perot-Fabry cavity formed by broadband Fresnel reflections from the PCF ends. With this configuration without selective mirrors, spectral broadening is found to influence laser power characteristics in a perturbative way which has never been found in RFLs made with FBGs. Our experimental setup is presented in Sec. 2 and the experimental and theoretical study of laser characteristics is presented in Sec. 3. Sec. 4 and 5 are devoted to the presentation of spectral and polarization characteristics of our laser, respectively.

2. Experimental setup

Our experimental setup is schematically shown in Fig.1. The pump source is a linearly-polarized Ytterbium-doped single-mode fiber laser operating at $\lambda_p = 1064$ nm. This laser has a linewidth of ~ 1.3 nm and a maximum cw output power of 20 W. The pump power launched inside the fiber can be adjusted by rotating a half-wave plate (HWP1) located before a polarizing cube. The pump power can also be slowly swept by rotating a motorized half-wave plate (HWP2) which is located before the Faraday isolator. The polarization direction of the incident pump field can be rotated with a third half-wave plate (HWP3).

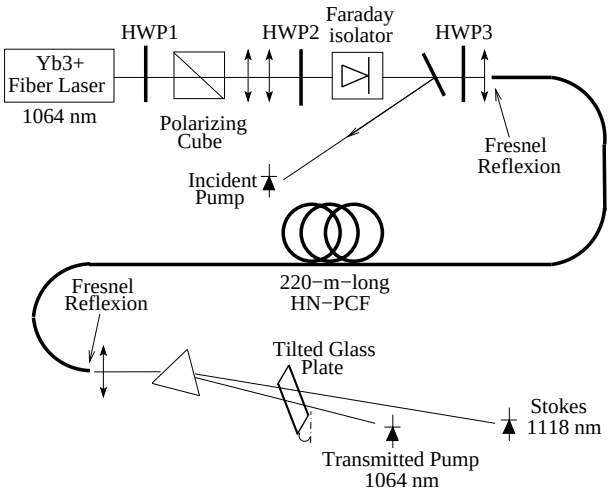

Fig. 1. Schematic representation of the experimental setup

#86993 - $15.00 USD Received 28 Aug 2007; revised 3 Oct 2007; accepted 3 Oct 2007; published 19 Nov 2007
(C) 2007 OSA

Our Raman active medium consists of a $\sim$ 220 m-long HN-PCF manufactured by Draka. The Raman laser oscillates within a Perot-Fabry cavity formed by the PCF cleaved ends which provide a broadband Fresnel reflection of 3.1%. This value of the reflectivity coefficient has been computed from the fiber effective index n_{eff} which is of 1.43 around the Stokes wavelength λ_s of $\sim$ 1118 nm. The germanium content in the doped section of the PCF core is about $\sim$ 25 Wt%. The geometrical core diameter is of about $\sim 2.5\ \mu$m. The zero dispersion wavelength of the PCF is around 900 nm which means that both pump and Stokes wavelengths are in anomalous dispersion region. The measured PCF losses at pump and Stokes wavelengths are $\sim$ 9.6 dB/km and $\sim$ 9.2 dB/km, respectively.

As shown in Fig. 1, the Stokes beam and the transmitted pump beam are spatially separated in free space by using one prism. A tilted glass plate corrects the anisotropic polarization transmission of the prism. The evolution of total Stokes and pump powers are recorded by two photodiodes which have a 200-MHz bandwidth. These two photodiodes are connected to a 200-MHz digital oscilloscope and a careful calibration procedure allows us to convert their output voltages into optical powers. The relative uncertainty on the measured values of the optical powers, resulting from uncertainty in the calibration procedure, is estimated to be less than $\sim$ 10%. Note that the evolution of the incident pump power is monitored by a photodiode detecting a small amount of light reflected by a glass plate located before the aspheric lens used to launch the light inside the PCF.

3. Laser characteristics

Laser characteristics recorded by sweeping the incident pump power at a few Hz are presented in Fig. 2. We will show in Sec. 5 that our PCF Raman laser behaves as a PMF Raman laser. This means that pump and Stokes waves can be linearly polarized along one of the PCF birefringence axes. All the results presented in the present Section correspond to this situation. This has been obtained from a careful optimization procedure in which the laser threshold has been adjusted at its minimum value by rotating HWP3. The angle θ_p between the polarization direction of the incident pump field and one of the birefringence axes is then equal to $0\,^\circ$.

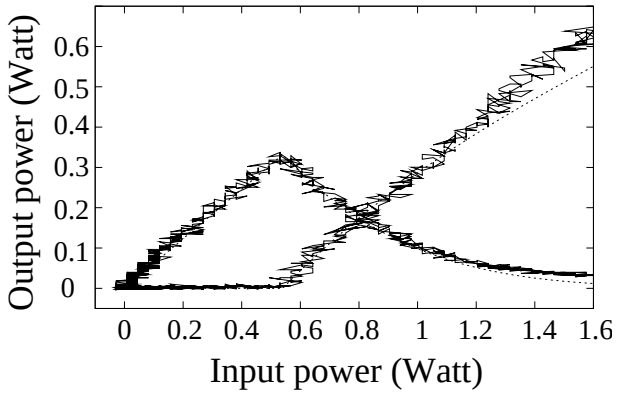

Fig. 2. Characteristics of the linearly-polarized PCF Raman laser ($\theta_p = 0^\circ$). The theoretical characterics are plotted in dashed lines with the following parameters: $\alpha_p = 2.21$ km^{-1}, $\alpha_s = 2.12$ km^{-1}, $G_R = 41.9$ km^{-1}W^{-1}, $R = 0.031$, $L = 220$ m, $\lambda_p = 1064$ nm, $\lambda_s = 1118$ nm. They nearly perfectly coincide with experimental characteristics except above $\sim$ 1.3 Watt.

Using the model proposed by Auyeung and Yariv [11], the value of the Raman gain in our PCF can be determined from the measurement of laser threshold power. Considering linearly-

#86993 - $15.00 USD Received 28 Aug 2007; revised 3 Oct 2007; accepted 3 Oct 2007; published 19 Nov 2007
(C) 2007 OSA

polarized optical fields, the usual stationary model consists of the three following ordinary differential equations governing the longitudinal evolutions of optical powers:

$$\frac{dP}{dz} = -\alpha_p P - G_R \frac{\lambda_s}{\lambda_p}(F+B)P, \tag{1}$$

$$\frac{dF}{dz} = -\alpha_s F + G_R P F, \tag{2}$$

$$\frac{dB}{dz} = \alpha_s B - G_R P B. \tag{3}$$

$P(z)$, $F(z)$ and $B(z)$ represent the pump wave power, the forward Stokes power and the backward Stokes power, respectively. α_p and α_s are the power attenuation coefficients at pump and Stokes wavelength, respectively. G_R is the Raman gain coefficient measured in $\mathrm{m}^{-1}.\mathrm{W}^{-1}$. To describe the stationary characteristics of the laser oscillating inside a Fabry-Perot cavity, these equations must be supplemented by the following boundary conditions:

$$P(z=0) = P_{inc} \tag{4}$$

$$F(z=0) = R\ B(z=0) \tag{5}$$

$$B(z=L) = R\ F(z=L) \tag{6}$$

where L and R represent the PCF length and the power reflectivity of the PCF ends, respectively. Considering that the pump wave is undepleted by Raman interaction at threshold, we obtain the following analytical expression for the laser threshold power:

$$P_{th} = \frac{\alpha_p[\alpha_s L - \ln(R)]}{G_R[1-e^{-\alpha_p L}]}. \tag{7}$$

The value of the reflectivity R computed from the fiber effective index is of 3.1% both at pump and Stokes wavelengths. Taking a threshold power P_{th} of 540 mW, we obtain a Raman gain G_R of 41.9 $\mathrm{km}^{-1}.\ \mathrm{W}^{-1}$ (or $G_R = 182$ $\mathrm{dB.km}^{-1}.\mathrm{W}^{-1}$) for co-polarized pump and Stokes waves. It should be emphasized that this value of Raman gain is 2.5 times greater than the value measured in the PCF Raman laser studied in ref. [9]. This can be explained by the high GeO_2 doping of our PCF core.

The numerical procedure used to solve Eqs.(1)-(6) is based on the Newton scheme implemented to find the value of $B(z=0)$ for which the function $B(z=L) - R\ F(z=L)$ vanishes to zero. For fixed parameters and for a given value of $B(z=0)$, Eqs. (4)-(5) provide the initial conditions required for the integration of Eqs. (1)-(3) from $z=0$ to $z=L$. The numerical integration of Eqs. (1)-(3) is performed by using a 8-order step adaptative Runge-Kutta method which gives the values of $F(z=L)$ and $B(z=L)$. The value of $B(z=0)$ is then modified according to the Newton scheme. The whole procedure is repeated until Eq. (6) is satisfied.

As shown in Fig. 2, lasers characteristics computed from the numerical integration of Eqs. (1)-(6) coincide quantitatively very well with characteristics experimentally recorded. In particular, a nearly full depletion of the transmitted pump power is observed for an incident pump power ~ 2.5 times greater than the threshold power. To the best of our knowledge, such a pronounced depletion of the transmitted pump power has only been observed in ref. [15]. In the laser of ref. [15], it arises from the use of broadband chirped FBGs with bandwidths of several nanometers. Even at high incident pump power, the width of the Stokes optical spectrum never exceeds the bandwidth of the chirped FBGs and the depletion of transmitted pump power is therefore fully effective [15]. Those circumstances are not found in most RFLs which are commonly made with FBGs having reflectivity bandwidths narrower than ~ 1 nm. At high pump

#86993 - $15.00 USD Received 28 Aug 2007; revised 3 Oct 2007; accepted 3 Oct 2007; published 19 Nov 2007
(C) 2007 OSA

power, the optical spectrum of these lasers does not remain bounded within the reflectivity spectrum of the cavity FBGs. As shown in Fig. 2(a) of ref. [16], this strongly reduces the depletion of the transmitted pump power. On the other hand, the bandwidth of our cavity mirrors (Fresnel reflections) is so wide that spectral broadening is not restrained by wavelength-selective optical elements and pump depletion is therefore fully effective. Let us emphasize that spectral features observed in our grating-free RFL strongly differ from spectral features observed in Raman lasers made with FBGs. These points are further discussed in Sec. 4.

The significance of the remarkable agreement found between experiments and theory deserves to be further discussed by putting emphasis on the situation of our result in proper context. Although the model introduced by AuYeung and Yariv in the 1970s is still commonly used nowadays to describe RFLs, it cannot be employed in most experimental situations because it forgives polarization effects and spectral broadening which are either unavoidable or uncontrolled in most experimental setups (see in particular ref. [16, 18] and references therein). In our study, the use of the scalar model by AuYeung and Yariv is fully justified because great care has been taken to ensure that light polarization is linearly maintained inside the PCF. In RFLs made with FBGs, spectral broadening has significant influence on the depletion of pump power. However most of the authors studying the characteristics of RFLs often ignore this point by restricting their work to the only examination of the laser characteristic associated to Stokes emission. To describe the fact that the laser optical spectrum becomes wider than the reflectivity spectrum of the output FBG, they compute an effective FBG reflectivity from an overlap integral between spectral power densities of incident and reflected beams [13–15]. This effective reflectivity depends on the incident pump power because the spectral broadening is itself function of power. Although characteristics computed from this procedure sometimes fit experimental curves [12, 15], it has been shown that this way to treat spectral broadening is not physically founded [16]. In the present work, Fresnel reflectivity coefficients of our cavity mirrors have been calculated from the effective index of the PCF. They are fixed parameters that do not change when P_{inc} is increased. In our work, a quantitative agreement between experiments and results computed from the usual model has therefore been obtained in a way which is physically founded and without the introduction of an unphysical effective reflectivity.

4. Laser optical spectrum

Our grating-free RFL can be seen as a new experimental tool for the investigation and the understanding of the formation of the optical spectrum in RFLs. Stimulated Raman scattering, optical Kerr effect and fiber chromatic dispersion are the three main physical effects determining the output spectrum of RFLs. In Raman lasers oscillating inside Perot-Fabry cavities closed by FBGs, these effects interplay within a wavelength-selective optical resonator confining Stokes spectrum within a bandwidth of ~ 1 nm centered around a well-defined wavelength. The theoretical question of the description and the analysis of spectral broadening occurring in RFLs made with FBGs is complicated and only a very few authors have attempted to tackle this problem [14, 19, 20]. Our grating-free RFL can be considered as a simpler system in which spectral features are not influenced by the presence of wavelength-selective mirrors. Understanding the formation and the evolution of the Stokes optical spectrum in a laser cavity made with broadband mirrors is a fundamental question which has not been much explored yet even though it could provide better insight into the physics of RFLs. In this Section, we investigate experimentally spectral properties of our grating-free RFL and we evidence some clear experimental signatures which have not been reported yet.

As shown in Fig. 3, increasing the incident pump power induces both a shift and a broadening of the Stokes optical spectrum. In addition with these two signatures, it must be noted that the shape of the Stokes optical power spectrum does not change and that it remains always well

#86993 - $15.00 USD Received 28 Aug 2007; revised 3 Oct 2007; accepted 3 Oct 2007; published 19 Nov 2007
(C) 2007 OSA

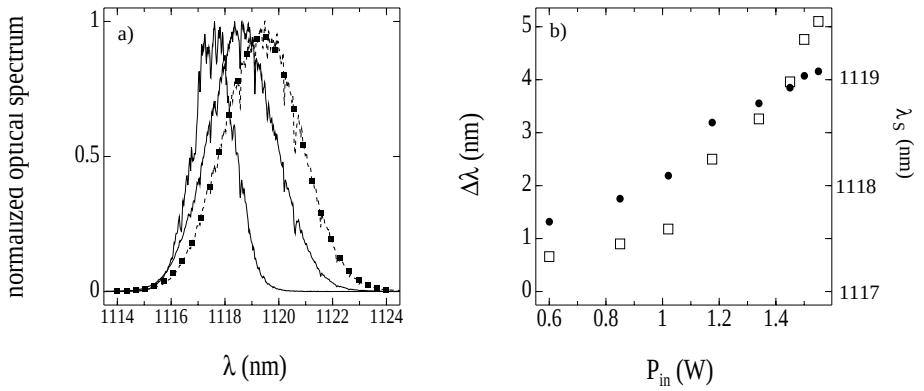

Fig. 3. (a) Normalized Stokes optical power spectra. Increasing the incident pump power ($P_{inc} = 1$ W, $P_{inc} = 1.35$ W, $P_{inc} = 1.5$ W), the shape of the Stokes spectrum remains Gaussian but its central wavelength exhibits a red shift while its width increases. The filled squares plotted on the spectrum centered around 1119.5 nm represent a Gaussian fit of the Stokes optical spectrum. (b): Wavelength drift and broadening of Stokes optical power spectrum with incident pump power. Open squares: Stokes central wavelength. Filled circles: full width at $1/e$ of Stokes power spectrum

fitted by a Gaussian function whatever the incident pump power.

All these features drastically contrast with those observed in RFLs made with FBGs. In FBG-based RFLs, the shape of the Stokes optical power spectrum usually continously change from a single narrow peak well-centered within the reflectivity spectrum of the FBGs to a double-peak characterizing the fact that the Stokes optical spectrum has became wider than the reflectivity spectrum of the FBGs at high pump power [12,16]. Moreover the central wavelength of Raman lasers made with FBGs does not drift with the incident pump power. It remains obviously well centered around the central wavelength of the FBGs. In our cavity without selective mirrors, the central wavelength for laser oscillation contrarily shifts continuously from ~ 1117.5 nm around threshold to ~ 1119.5 nm when the incident pump power is increased from threshold to 1.6 Watt. The full-width at $1/e$ of the Stokes optical spectrum simultaneously increases from ~ 1 nm to ~ 4 nm (see Fig. 3(b)). Let us emphasize that our pump laser is properly isolated from the Raman fiber laser. In our setup, the pump wavelength remains well fixed at 1064 nm and the drift of the Stokes wavelength is not due to the drift of the pump wavelength, in strong contrast with results presented in ref. [6].

Our results show that spectral broadening in RFLs oscillating in a cavity made with broadband mirrors is qualitatively very different from spectral broadening occurring in Raman fiber lasers made with FBGs [16]. In particular, the absence of FBGs reveals a drift of the Stokes wavelength with incident pump power which has never been observed before. Moreover the Stokes optical power spectrum presents a Gausssian shape which remains invariant with the input power. The experimental signatures characterizing the evolution of the optical power spectrum in our grating-free RFL are therefore rather simple and clear. However further theoretical work is indispensable to understand spectral features observed in experiments.

An original theoretical analysis based on kinetic wave equations has been recently applied in a RFL oscillating in a high finesse cavity [19, 20]. This approach has been found to provide a good description of the hyperbolic secant shape characterizing the spectral output of this specific laser whereas the shape of our laser optical power spectrum is Gaussian. The approach presented in ref. [19, 20] cannot be straightforwardly applied to our laser which oscillates in

#86993 - $15.00 USD Received 28 Aug 2007; revised 3 Oct 2007; accepted 3 Oct 2007; published 19 Nov 2007
(C) 2007 OSA

a low-finesse cavity around a wavelength which is far from the zero-dispersion wavelength of the PCF. It should be noticed that further modeling must take into account the fact that spectral effects observed in our laser have only little influence on the laser power characteristics. Finally theoretical investigations made by Stolen about spectral development of stimulated Raman scattering in optical fibers should also be considered as preliminary guiding steps for the study of the shift of the Stokes central wavelength with incident pump power [21]. However careful measurements of the Raman gain and losses spectra of our HN-PCF must first be made. These spectra should actually differ from the usual gain and losses spectra of standard fibers and their determination is clearly needed for the good understanding of the spectral properties of our grating-free RFL.

5. Polarization effects

Rotating the polarization direction of the incident pump field by $\sim 45^\circ$ from the situation illustrated in Fig. 2(a) induces nearly a doubling of the laser threshold power illustrated in Fig. 4. This behavior already observed in various PMF Raman lasers [17, 18, 22, 23] typifies undoubtedly a Raman laser oscillating in a highly birefringent fiber. With high values of the fiber birefringence (typically of the order of $\sim 10^{-4}$), a RFL consists of two independent Raman lasers linearly polarized along the birefringence axes [18]. Rotating the polarization direction of the incident pump field amounts to distribute the incident power between two lasers which have identical threshold because they oscillate within the same cavity. When the angle θ_p between the polarization direction of the incident pump field and one of the birefringence axes is equal to $\sim 45^\circ$, the incident power is equally splitted along the two birefringences axes. The pump power indispensable to initiate Stokes oscillation in two independent lasers is then simply twice the pump power required to initiate the oscillation of only one laser linearly polarized along one of the birefringence axes. The structure of our PCF has been designed without mapping any stress anisotropy but this sensitivity of laser characteristics to light polarization probably arises from a strong shape birefringence due to distorsions in the geometry of the fiber cross-section [24]. In summary, the dependence of threshold power and laser characteristics to light polarization (see Fig. 2 and Fig. 4) proves that our RFL oscillates within a fiber in which polarization modes are decoupled. This means that the value of the PCF birefringence may be of the order of $\sim 10^{-4}$ [18].

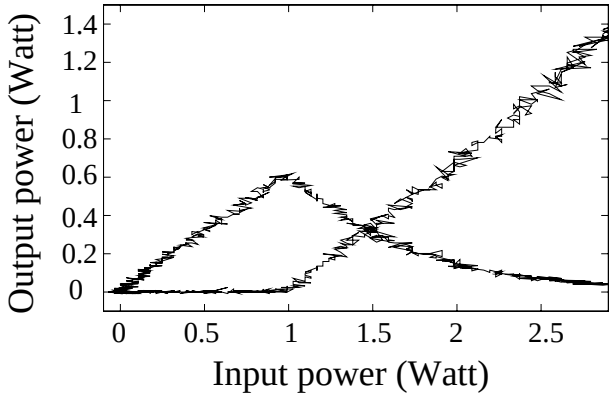

Fig. 4. Influence of polarization direction of the incident pump field on laser characteristics. The angle θ_p between the incident pump field and the birefringence axes is of $\sim 45^\circ$ which induces doubling of the laser threshold power (see Fig. 2 for comparison).

The previous argumentation is strengthened by the fact that out PCF Raman laser delivers a

#86993 - $15.00 USD Received 28 Aug 2007; revised 3 Oct 2007; accepted 3 Oct 2007; published 19 Nov 2007
(C) 2007 OSA

Stokes beam devoided of temporal instabilities. In RFLs made with standard fibers, the birefringence is so weak that the two fibers polarizations modes are coupled by Raman and Kerr effects. This can result in the emergence of self-oscillations of the output Stokes power [22]. On the other hand Stokes emission is always stable in Raman lasers made with PMFs because the birefringence is so high that fiber polarization modes are uncoupled [18, 22].

The discussion given above shows that our PCF Raman laser behaves a Raman laser oscillating in a polarization maintaining single-mode fiber. However small quantitative differences must be mentioned. First of all, the polarization extinction ratio of the pump and Stokes waves at the laser output is around $\sim 10\%$. This might be imputed to a birefringence value lower than 10^{-4}. However we estimate that this is rather due to the presence of a higher-order transverse mode. This may explain the fact that the threshold power is multiplied by a factor of 1.85 instead of a factor 2 when polarization direction θ_p is rotated from 0° to 45°. However the possible presence of several tranverse modes seems to be perturbative since experimental characteristics are remarkbly well fitted by a single mode model.

6. Conclusion

We have demonstrated a Raman laser made from a PCF exhibiting a Raman gain so high that Stokes oscillation can be initiated inside a Perot-Fabry cavity only formed by weak broadband Fresnel reflections from the fiber ends. The physics of this laser has been studied by putting emphasis on the comparison with Raman lasers oscillating in Perot-Fabry cavities closed by FBGs. In our laser with broadband mirrors, the Stokes optical spectrum has been shown to broaden with the incident pump power while its central wavelength continuously drifts and its shape remains invariantly Gaussian. These spectacular spectral effects have been found to influence the laser power characteristics only in a pertubative way. The model introduced by AuYeung an Yariv is thus found to describe the laser power characteristics in a quantitative and accurate way without any phenomenological adjustment of physical parameters, as it is usually done in Raman lasers with FBGs. Considering the influence of light polarization, the power characteristics of our PCF Raman laser have been found to exhibit features similar to those already observed in Raman lasers made with PMFs. The possible existence of a strong shape birefringence arising from distorsions in the geometry of the PCF cross-section has been proposed to explain the fact that our Raman laser undoubtedly oscillates in a highly birefringent fiber.

Understanding the formation and the evolution of the Stokes optical spectrum in RFLs is a fundamental question which has not been much explored yet. Our demonstration of a RFL oscillating in a laser cavity made with broadband mirrors and our experimental study of its spectral properties sketches out new directions for further theoretical investigations on spectral properties of RFLs. Further studies on the influence of the emergence of higher-order Stokes components on the dynamics and the spectral properties of our grating-free RFL are also currently in preparation.

The Centre d'Etudes et de Recherches Lasers et Applications is supported by the Ministère chargé de la Recherche, the Région Nord/Pas de Calais and the FEDER. This work was supported by the EU framework 6 project "NEXTGENPCF".

#86993 - $15.00 USD Received 28 Aug 2007; revised 3 Oct 2007; accepted 3 Oct 2007; published 19 Nov 2007
(C) 2007 OSA